Additive Manufacturing for Complex Structures with Magnetic Smart Materials

Undergraduate Honors Research Thesis

Presented in Partial Fulfillment of the Requirements for

Graduation with Distinction in the

Department of Mechanical Engineering at

The Ohio State University

By:

Brandon Cruz

May 2021

Advisor: Professor Ruike (Renee) Zhao, Ph.D.

Abstract:

Stimuli responsive materials have shown great potential in the ability to add functionality to designs to achieve and complete certain tasks. While not ubiquitous, applications so far have been found in fields of soft robotics in the case of mechanical grippers to drug delivery for minimally invasive surgeries. These materials operate by exhibiting certain mechanical properties once under the stimulation from an external stimulus. In the case of Magnetic Shape Memory Polymer (M-SMP), it responds with a combination of magnetic field intensity and direction along with temperature control to allow shape locking and unlocking below and above the glass transition temperature, respectively. Current fabrication methods inhibit the ability to combine functional ability of configurable mechanical properties with functional designs such as those used in springs. In this thesis, a method of 3D printing, Digital Light Processing (DLP), is explored as an avenue to develop and characterize feasibility and quality of printing custom complex millimeter-scale components. In developing a custom DLP enabled setup, formulating photosensitive m-SMP resin, and demonstrating functionality combined with various complexity, it is shown that it is possible to combine design complexity with material functionality. This research effectively expands the ability to apply complex geometric designs that can be manufactured and allows a fuller range of ability of fabricated parts.

Acknowledgements:

This year was full of challenges – some good and some difficult. I want to thank Dr. Ruike (Renee) Zhao for allowing me the opportunity to undergo a fulfilling challenge in completing research in her lab. Continuing my education is something important to my family and I, so in you being an understanding and supportive mentor through this process has been immense. I am looking forward to paying that back.

I want to thank Shuai Wu for him dedicating time to helping develop my skills in the SIM Lab. His support and willingness to answer all my questions as well as teach me to operate a lot of the tools in the lab helped advance my research at a rate that would not have been possible independently. The same is with Dr. Qiji Ze who has been supportive and friendly as well as willing to identify other potential projects and areas that can benefit me in my work in the lab.

I want to thank my friends who for the countless number of years have been faithfully at my side and constantly pushing me to do my best. Having a family away from home has been a large underlying difficulty for me and knowing your support has culminated in this project has made me proud to dedicate this. It would not have been nearly as possible without you all.

I want to thank Ruhani, my beautiful girlfriend, for being so resilient in the times I had much to do and not a lot of time to spare. She never thinks any challenge is above me, and she always reminds me that I can do anything I can put my mind to. This accomplishment is for us just as anything else we do together. I love you.

For my parents and brothers, I feel such emotion writing this paragraph because I know you all are proud to see me succeed. Ever since I was small, you all instilled in me how capable I am of anything even when I did not know. Now, I believe this, and it is this amazing gift that you all have given me which has allowed me to succeed. Cada cosa que logro a ustedes se la dedico.

Contents

List of Figures

List of Tables

Chapter 1: Introduction

Materials have an important and complex role in engineering. They are the basis with which designs are based off. In recent years, special interest has formed for materials that respond to stimuli to achieve physical and chemical temporal changes [9]. These materials, known as smart materials, achieve their intended functions from external stimuli like those found in nature – temperature, light, chemical changes, magnetic fields, etc. Due to the flexibility in design provided by the increased functionality, there are several fields that smart materials provide useful benefits. In the broadest sense, soft materials such as those actuated magnetically can reconfigure their shapes while in the presence of the magnetic fields. As the shape morphing is applied, such as in locomotion, dynamic motion is used for navigation for intricate motions like rolling, jumping, and even crawling [2]. Alternate applications with which these smart materials are used is in spaces such as for sensors, generation of heat, and manipulation of objects. As these materials are developed and refined, there is an increasing scope for which smart materials may be applied in engineering.

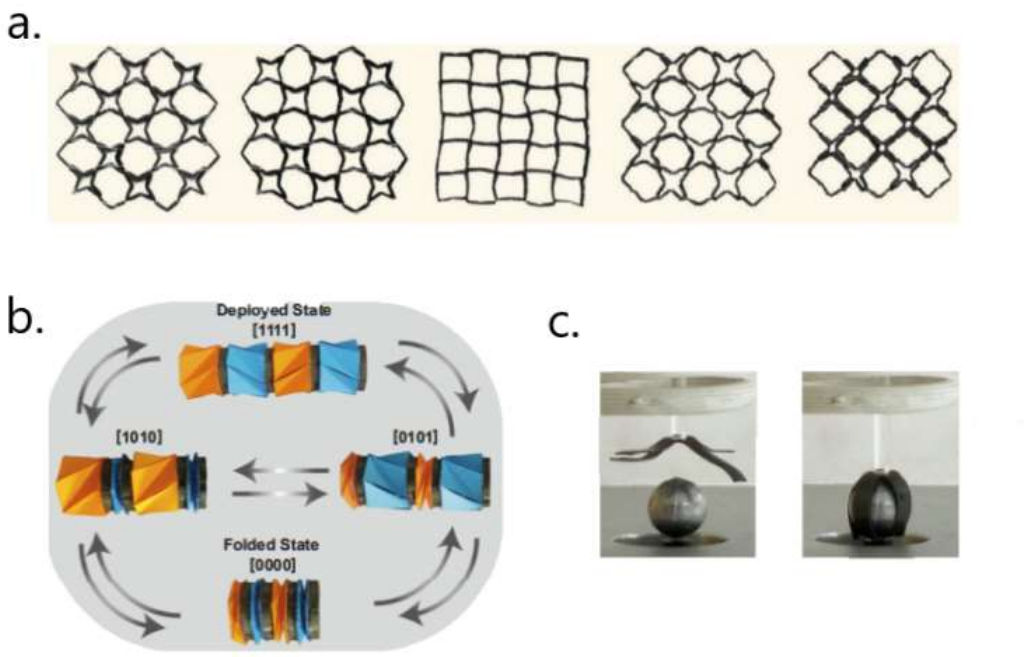

Figure 1: a.) Magnetically actuated metamaterial array in variety of deformation modes (Adapted from [10], Advanced Functional Materials) b.) Sequential magnetic actuation of Kresling origami patterns (Adapted from [28], Proceedings of the National Academy of Sciences) c.) Magnetic Shape Memory Polymer gripper picking up lead ball (Adapted from [3], Advanced Materials)

Widespread traction has been gained to implement smart materials since they respond to natural stimuli as well as in some cases respond to multiple stimuli. In the figure above, a variety of applications are shown in various research capacities which vary from shape configuration (Figure 1a.), object manipulation as seen in torque response of Kresling origami unit cells (Figure 1b.), and response to multiple stimuli in combination such as temperature and magnetic field to grip and shape lock (Figure 1c.).

These smart materials exist in several compositions: soft hydrogels, soft elastomers, and shape memory polymers (SMPs) among others. Shape memory polymers are of particular interest in smart material research due to the unique ability to memorize shapes temporarily and reconfigure to its permanent shapes when exposes to external stimuli [1]. SMPs are generally stiffer than other soft matrix composites allowing applications in fields of medicine such as

biomedical devices for drug delivery or even within soft wearable technology and sensors [3, 26].

As there exist several metamaterials that are used in these applications, there are rapidly growing numbers of types. One material combination involves hard-magnetic particles embedded in SMP matrix which lack the ability to remain magnetized under external magnetic fields. Due to this, these hard-magnetic particles are magnetized to saturation with high magnetization. This allows the lower applied magnetic field to induce micro-torques in the material system as a function of torque per volume. The configuration also supports more sustainable magnetic materials through these embedded hard-magnetic materials.

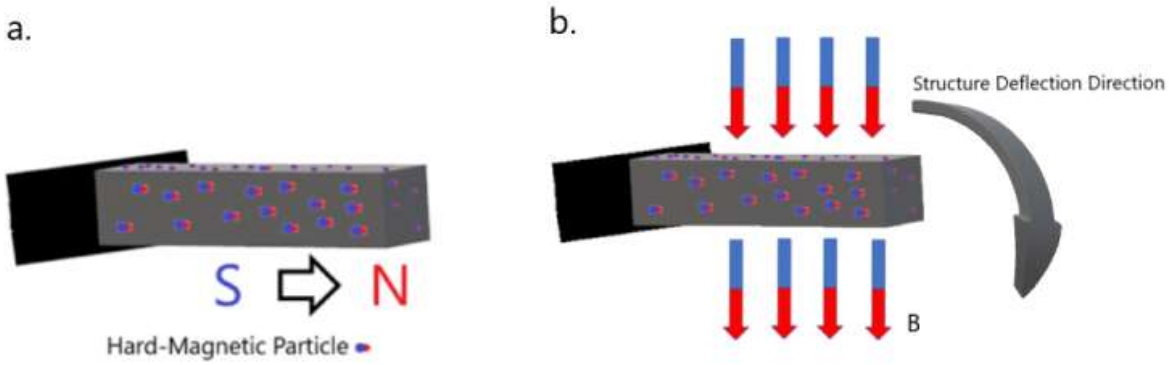

Figure 2: a.) SMP matrix with embedded hard-magnetic particles b.) Actuating mechanism of hard-magnetic composites

In recent work, research has been done to develop embedded hard-magnetic materials, neodymium-iron-boron (NdFeB) and iron-oxide (Fe_3O_4), into an amorphous acrylate-based shape memory polymer matrix. This material is known as magnetic shape memory polymer (M-SMP) [3,4]. The polymer matrix acts as a soft, deformable material with embedded magnetized NdFeB that interacts with the actuating magnetic field to induct the shape configuration while.

Below the T_g, the matrix exhibits high stiffness prohibiting shape transformation, so the iron-oxide embedded in the matrix interacts applies induced heating through separate magnetic actuation. In these efforts, the M-SMP material is developed through an additive manufacturing process known as direct-ink writing (DIW). Here the magnetic material system is fabricated by extrusion out of a syringe, and a magnetic ring attached to the nozzle guides the particles out of the syringe as a pattern defined previously before curing the material under UV light [4]. The M-SMP material shows great promise in its ability to have untethered control through magnetic field, and its ability to shape lock and reconfigure its shape, allowing applications in many areas.

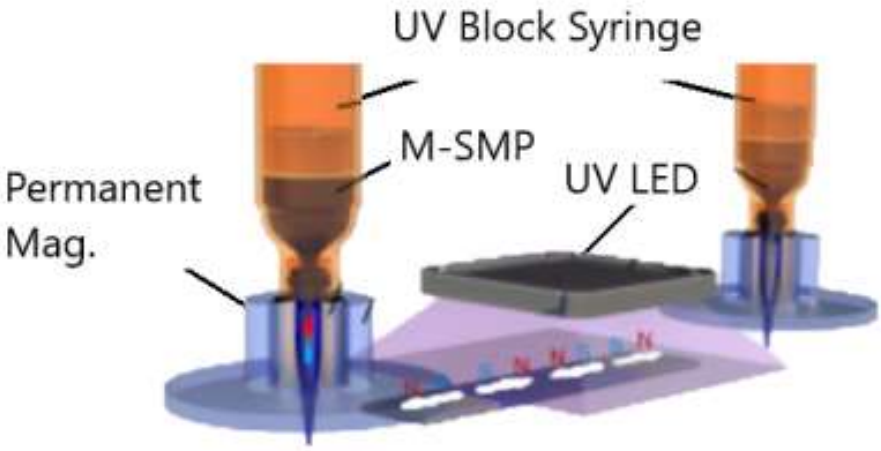

Figure 3: Direct Ink Writing Setup used to fabricate M-SMP structures (Adapted from [3], ACS Applied Materials & Interfaces)

This method of manufacturing is used to print simple structures but lacks the ability to develop complex geometries. The resolution is severely limited by the nozzle and its ability to print finer extrusions. Because of this, the DIW method of producing M-SMP is limited to its current state. A secondary method of producing M-SMP is using dissolvable molds. The molds determine the net shape of the component, and the material resin is injected into the mold before

being heat-cured and dissolving the mold in water. Other methods of additive manufacturing used for fabricating involve processes such as FDM [18 - 20], stereolithography (SLA) [23-25], and other integrated techniques [21]

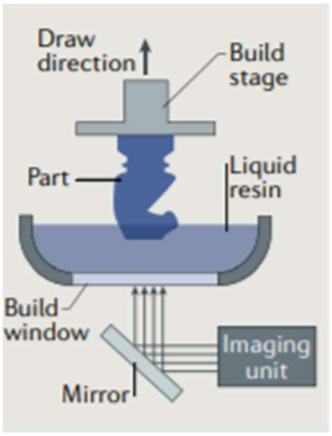

Figure 4: Standard setup and components of DLP printer (Adapted from [5], Nature Reviews | Materials)

Due to these restrictions in the ability to fabricate complex geometries with high resolution, a different method of fabricating the M-SMP is necessary. A unique additive manufacturing method to the previously mentioned DIW for fabricating these materials [16,17] is digital light processing (DLP). This resin method of 3D printing functions by using a light source, projector, to selectively cure material precursor on a layer-by-layer basis connected to a base material and lifted out of the resin bath to create a solid object [5]. DLP allows complex geometries to print from the resin. The mechanism of operation is like that of SLA [23 – 25]. With the ability to produce higher resolution components, the benefits will allow parts with millimeter-scale to be produces in an expedited manner and high efficiency for quicker turnaround and less waste of material. Higher complexity as defined by CAD models and ability to translate to the light source enables highly functional designs.

1.1 Focus of thesis

The objective throughout the project life cycle was to develop a process that would be able to combine Digital Light Processing with the Magnetic Shape Memory Polymer material to effectively fabricate parts with high functionality and resolution while maintaining small scale (millimeter). The focus of the project is to optimize and define the parameters of the DLP system that can enable the material precursor with specified tunable properties to be developed into a complex structure like that of a real-world application. This project commanded heavy focus of engineering fundamentals, knowledge of machine design, measurements, and domains such as mechanics of materials as well as data analysis to robustly produce a highly functioning process for fabricating M-SMP into a variety of small, complex structures.

1.2 Significance of Research

Smart materials increasingly will become popular in usage as they continue to demonstrate unique capabilities beyond that of traditional materials. As they continue this expected trend, there is demand within drug delivery to utilize soft robots to enter non-invasively into the human body to deploy drugs as signaled by certain stimuli from the target area. In the case of magnetically controlled material, it is possible to control these mechanisms without the need for entering the body.

With the advancement of DLP for use with M-SMP, it is possible to create more complex structures that allow the fabrication of soft robots with indistinguishable functional components. The high resolution of the fabricated parts enables precise functions such as locomotion, or configuration into functional objects as in the case of grippers [27].

The optimization of the parameters that allow the successful DLP fabrication of M-SMP are significant in that they will determine a successful method with which to print the material and provide insight to enable other magnetic material to be developed via DLP.

1.3 Overview of Thesis

The thesis consists of major chapters involved in conducting the research project. Chapter 2 provides an overview of the development and components used in a custom-made DLP setup. The mechanism of printing is also discussed as it relates to M-SMP and generating 3D printed parts.

Next, formulation of the DLP-compatible resin is explored, and various compositional combinations are experimented to tune specific properties to enable successful printing and curing of the resin layer by layer. Beyond specific resin properties, characterization of these properties is determined to baseline performances of each combination.

From down selecting a viable resin composition, the material is then used to develop and print functional parts that can demonstrate the ability of M-SMP to combine stimuli-responsiveness with complexity of design. Characterization of the development of printed parts is done so by examining mechanical properties as well as quality of actuation and dimensional integrity.

Finally, the conclusion will discuss in summary the key points and contributions because of the research project and touches on applications made possible from the scope of this work. Future work and recommendations will also be included.

Chapter 2: DLP Printer Setup

The mechanism by which the M-SMP is developed by is Digital Light Processing (DLP). DLP is a method of light processing like that of stereolithography (SLA), but it differs in that SLA cures a single “voxel” from a point-source and DLP projects the sliced mask pattern across the tank layer by layer. As such, the time cost in fabricating components through DLP is much lower than that of other additive manufacturing methods [6]. For use throughout the project, a custom built DLP printer is employed rather than commercial. The custom printer allows for significant ability to be able to tune and control printing parameters relevant to the print process to optimize with the unique nature of the materials being developed.

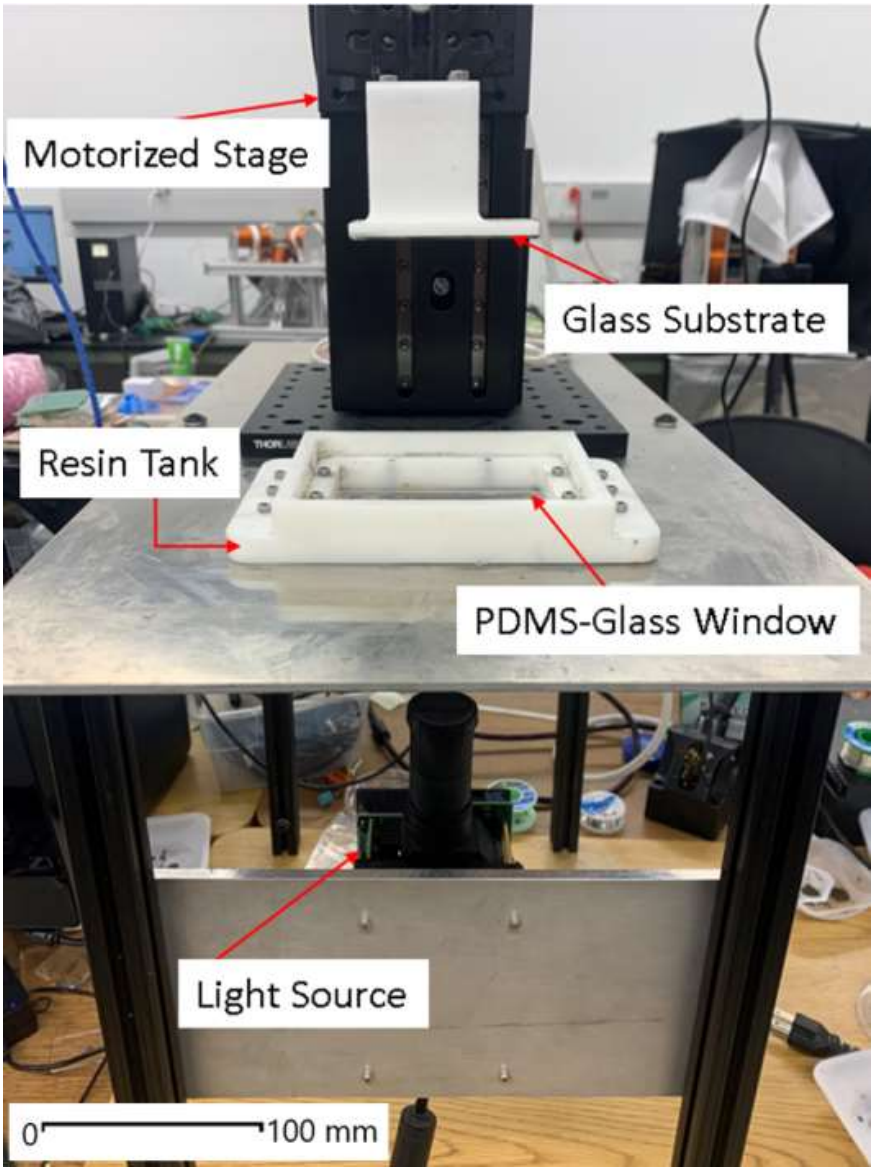

Figure 5: Image of custom DLP setup and major components found in SIM Lab

There are two configurations in which DLP can be constructed to print parts. Bottom-up mechanisms utilize a configuration where the projection of the system is below the tank, and the cured resin is translated in the z-direction upwards to maintain continuous addition of cured material. In a top-bottom configuration, the manner of setup is in the opposite direction with the projector field of view facing downwards towards the tank. Bottom-up systems for DLP are

widely utilized and preferred for their benefits when compared with top-bottom configurations [7].

The working mechanism which the custom-made DLP system produces printed parts uses a Wintech PRO4500 LED projector with a dominant wavelength of 385 nm. This device produces approximately 150 lumens at 15-W LED power consumption and sits at the base of the DLP system acting as the light source to which the photosensitive resin is cured [8].

The tank itself is 3D printed with length (71.36 mm), width (91.89 mm), and depth over 13 mm. To construct the tank bottom, a transparent window which can allow detachment of the freshly current layer, an acrylic perimeter which allows polydimethylsiloxane (PDMS) to be cured inside the tank area is formed above a glass window. This allows the substrate which the cured material is cured on to maintain relatively flat surface and detach from the PDMS. The PDMS itself is made from Sylgard 184 silicone elastomer base as well as Sylgard 184 silicone elastomer curing agent at a ratio of 5:1 of base to curing agent.

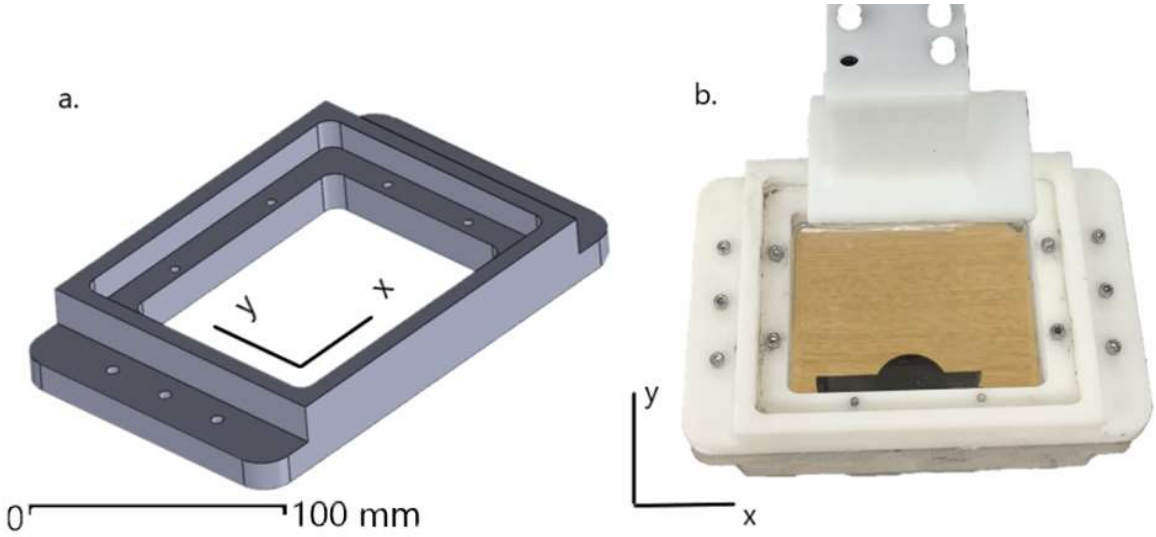

Figure 6: a.) CAD model of resin tank next to b.) assembled projector-window-tank

A moving stage is also necessary to provide translation in the z-axis and allow the printed material to expand vertically. A Thorlabs LTS150 150mm Stage is used as well as a LTS Series Motorized Stage. A motorized stage allows precise control over the location and speed of the substrate as it changes positions frequently and interacts with the tank surfaces. As such, attached to the motorized stage is a glass substrate to create high detachment force from the tank bottom. Commercial printers whether bottom-up or top-bottom function by continuous elevation or de-escalation. The custom DLP setup works similarly in that it takes a stepped approach by being calibrated to a zero-point just contacting the window, then each subsequent layer will cure for the desired time before the image is shut off at which point the moving stage translates upwards but returns to a point one layer thickness above the previous step. This allows the material to cure in a stepped fashion for each layer of the structure.

With the development of the DLP printer, custom parameters require tuning to be able to produce a functional printed part. These parameters associated with the print process vary with specific materials, and the same is done with M-SMP as well. In general, print process parameters which are tunable include the following [7,9]:

Table 1: DLP Parameters affecting print quality

Parameter #	Attribute Name	Variable (y/n)
1	Exposure Time	y
2	Curing Time each layer	y
3	Layer Thickness	n
4	Orientation	y
5	UV Intensity	n
6	Wavelength	n
7	UV Light Source	n

Each of these parameters are tunable within the custom-made DLP, yet to maintain within the scope of the project, the only variable print parameters will involve exposure time, curing time for each layer, and orientation of geometries for the sliced CAD file being processed (Parameters 1,2,4). The other parameters are consistent throughout the investigation and maintained through each test and trial. Beyond the optimization of these print process parameters, formulation of the DLP resin is also a large factor in the successful printing of a structure.

Chapter 3: Formulation of DLP Resin

Based on the conclusion of the development of the DLP printing system, the material precursor of the M-SMP was needed to be developed. The process in which the resin of the DLP precursor contrasts greatly to the precursor for M-SMP currently used. Due to this, only certain features of the material would be considered with the remainder of the characteristics and success criteria based on the performance of the printability of the new material.

Factors considered to determine how to formulate the DLP M-SMP resin included the functional ability of the magnetic material and ensuring sufficient particle loading of the magnetic material (NdFeB). A core component of the magnetic smart material is the presence of the hard magnetic particles present to contribute micro-torques throughout the printed part while under magnetic stimulation. Without compromising the quality and ability of the DLP curing, NdFeB must be present to deliver comparable magnetic actuation ability.

Special considerations are taken to develop a material that can maintain homogenous particle loading of the NdFeB to maintain functionality. With respect to the printing quality, the density must also be investigated to enable adequate fill time of the material between each layer of printing. Without proper filling of the tank with the displaced material, the subsequent layer meant to be cured would not have enough material to reach the layer thickness. As such, a balance of developing a material that can encompass the DLP tank in reasonable fashion and one which can maintain a degree of homogeneity must be taken.

To develop an actual structure through DLP, the curability of the M-SMP precursor is the biggest determinant of whether a print is possible. Due to the presence of additives relative to the printable resin, the quality of the print is dependent on the ratio and amount of core substance to

not be inhibited by the additives. This includes especially the use of photo absorbers. This additive is crucial to the ability of the resin to respond to light to initiate the polymerization process. In the context of printing components through DLP, these additives directly contribute to the cure depth as well as limiting a phenomenon called "overcuring" where an unintended amount of material is cured distorting the desired geometry.

By taking these factors into account among others an initial formulation is made to improve upon. With this formulation, iterative experimentation is done to improve each component not fixed. In the following table, the initial formulation of ingredients is shown as well as their contribution to the overall composition of the DLP precursor for M-SMP.

Table 2: Components to consider in M-SMP resin for DLP

Attribute	Cross-linker	Monomer		Initiator	Photo absorber	Viscosity Modifier	Hard Magnetic Particle
Component	AUD8413	IOA	PEA	819	Sudan II Fe_3O_4	SiO_2	NdFeB (100 μm)

Like that of other M-SMP recipes, the amount of cross-linker and monomer added are core substances in the formulation while the amount of initiator, photo absorber, viscosity modifier, and hard magnetic particle are additives which give the shape memory polymer its distinct characteristics.

In investigating the optimized formulation to be compatible with the custom DLP system, it is important to be able to measure and characterize success as well as benchmark milestones. Without many direct tools and processes in place to quantify specific attributes or characteristics of the formulation, it is crucial to measure what can be measured and reliably as well. For this reason, it was decided that the curability would be an important signal marker in the success of a

specific recipe of precursor. As mentioned in Table 1, layer thickness is a print process parameter directly dependent on the amount of material that can be cured to fulfill the layer size specified. Controlling curability of the precursor then allows other print process parameters to be manipulated if good enough. Managing this parameter also implies a control of the overcuring mentioned previously.

A process for measuring the cure depth and quality was used to ensure consistent results through each test. A droplet of each trial formulation is placed onto a transparent glass slide and placed into the DLP tank where an image is shown for a known amount of time. In this way, the geometry of the cured material is known as well as the amount of time exposed to the light in the tank. A standard simple design is used by flashing a slide of a series of 1 mm bars (white spacing is intended geometry). Coming from below the tank, the light is emitted onto the tank window and onto the droplets of material. With varying amounts of time, the behavior of the resin can be interpolated to understand the optimal amount of time to cure for a specified layer thickness. Also, the degree of the overcure can be measured by the amount of material between the intended geometry.

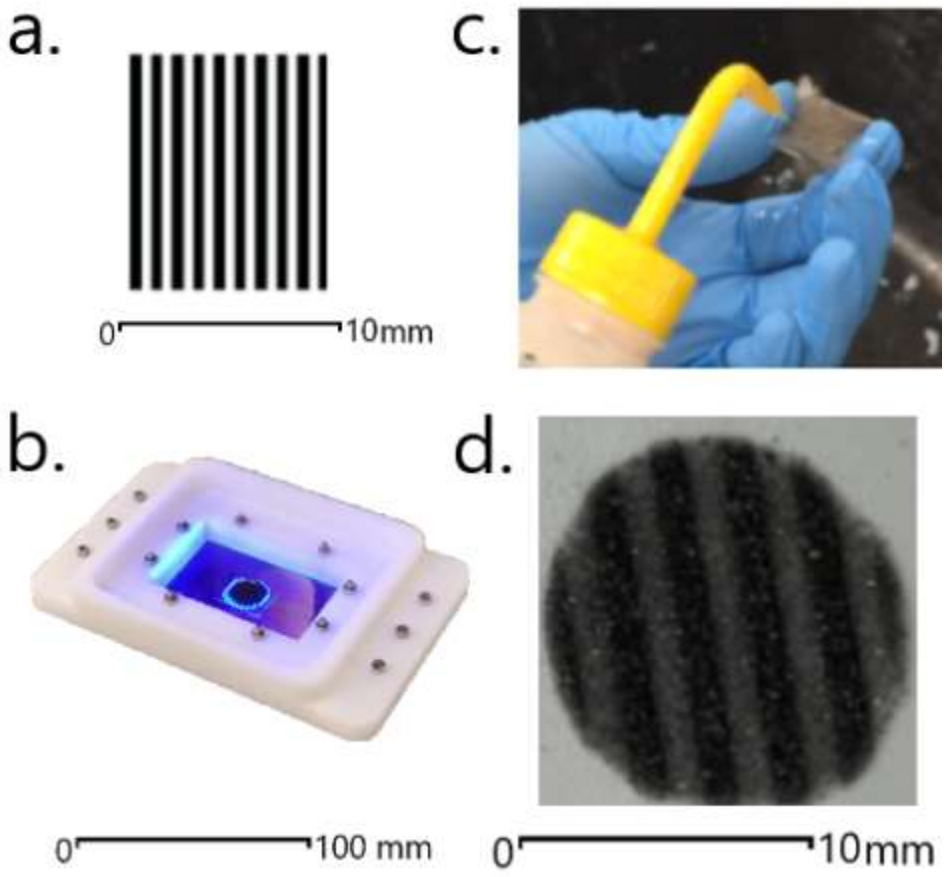

Figure 7: a.) Geometry of cure depth test design (1 mm bars) b.) Glass slide exposed to test geometry with test resin c.) Excess uncured material being cleaned after exposure d.) Final outcome to be measured and analyzed for cure depth test

The process is shown above is done for each new formulation which involves selecting the geometry (1mm bars), placing a droplet of precursor onto a glass slide and into the DLP tank before shining the geometry onto the slide for a specified amount of time, and eventually cleaning and measuring the slide to understand its cure time profile. A measurable criterion for understanding an adequate curing profile is for the resin in question to have at least twice the cure depth of the desired layer thickness. Throughout the course of the project, a layer thickness of 0.05 mm is used as a standard layer sizing. Using this size, the minimum cure depth allowable to be considered a successful dimension is given by:

$$Cure\ Depth \geq 2 * t_L\ (where\ t_L = Layer\ Thickness\ [mm])$$

$$Cure\ Depth \geq 2 * 0.5\ mm \geq 1.0\ mm$$

The density of the precursor as it relates to fill time was investigated primarily qualitatively. In a formulation of the M-SMP, a preliminary qualitative metric involved the ability to maintain homogeneity throughout the volume of resin. The viscosity modifier played in important role in allowing the hard magnetic particles to remain somewhat uniform throughout. The other qualitative metric in determining proper density was the fill time of the DLP tank. Depending on the speed and the distance of travel the moving stage would exhibit influenced the need for the fill time. With shorter distance traveled at a high rate, the resin would need to fill in a relatively short time compared to a large distance and slower rate of travel.

Table 3: Resultant formulation of DLP M-SMP resin and associated fractions

Attribute	Cross-linker	Monomer		Initiator	Photo absorber	Viscosity Modifier	Hard Magnetic Particle
Component	AUD8413	IOA	PEA	819	Fe_3O_4	SiO_2	NdFeB (100 μm)
Mass % (Volume %)	20	50	30	1.5	0.4	2.5	(10)

Through experimentation, the above formulation for the material precursor of M-SMP was found. The two proposed photo absorbers were incorporated into the resin and compared to one another, and after comparison of the resin being all things equal, the iron oxide additive was found to be more effective in reducing the overcuring effect as well as increasing the cure depth effectiveness.

The viscosity of the resin found to give best results in terms of achieving low refill time of the DLP tank as well as maintaining uniform distribution of the magnetic particle loading was

found at 2.5% mass volume. In this way, the resin would be able to take the shape of the tank volume as well as cure with consistent particle mass throughout the structure.

Using 0.5 mm layer thickness and the associated critical cure depth of 1.0 mm as the metric to compare test results, the following cure depth graph was found. Times less than 10 seconds were trialed to view realistic layer exposure conditions. The maximum depth found at 10 seconds of exposure is 0.23 mm which is twice as high as the critical cure depth noted in the chart. At low times (t = 3s), the cure depth is also above the threshold allowing for shorter exposure times and ultimately enabling faster DLP prints.

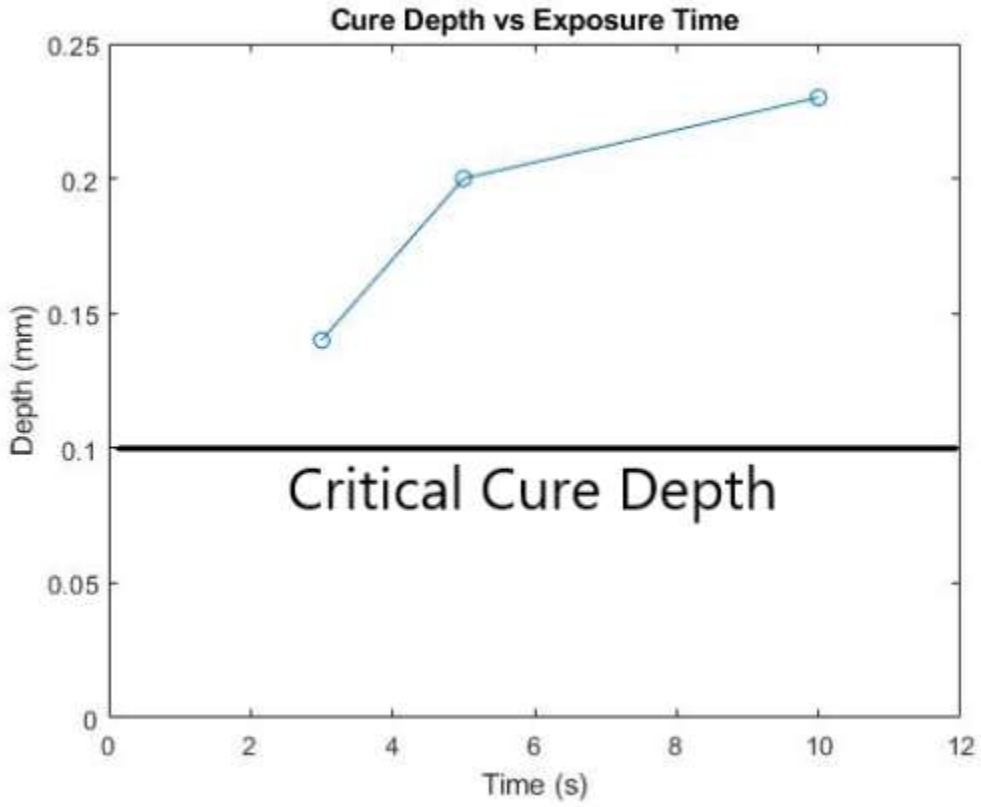

Figure 8: Cure Depth (mm) response across Exposure Time (mm)

To understand the behavior of the material as it transitions from temperature extremes, the dynamic thermomechanical properties are measured. This is done using a dynamic mechanical analysis (DMA) tester using DMA 850, TA Instruments, New Castle, DE. The temperatures are varied from room temperature (22 ℃) to elevated temperature well past the glass transition temperature (110 ℃). Thin strips of printed material from the formulation are developed with dimensions (approximately 10 mm x 2.6 mm x 0.6 mm). The strain used for the samples is oscillated with a frequency of 1 Hz and a peak-to-peak amplitude of 0.1%. The temperature is also swept at a rate of 3 $\frac{℃}{min}$.

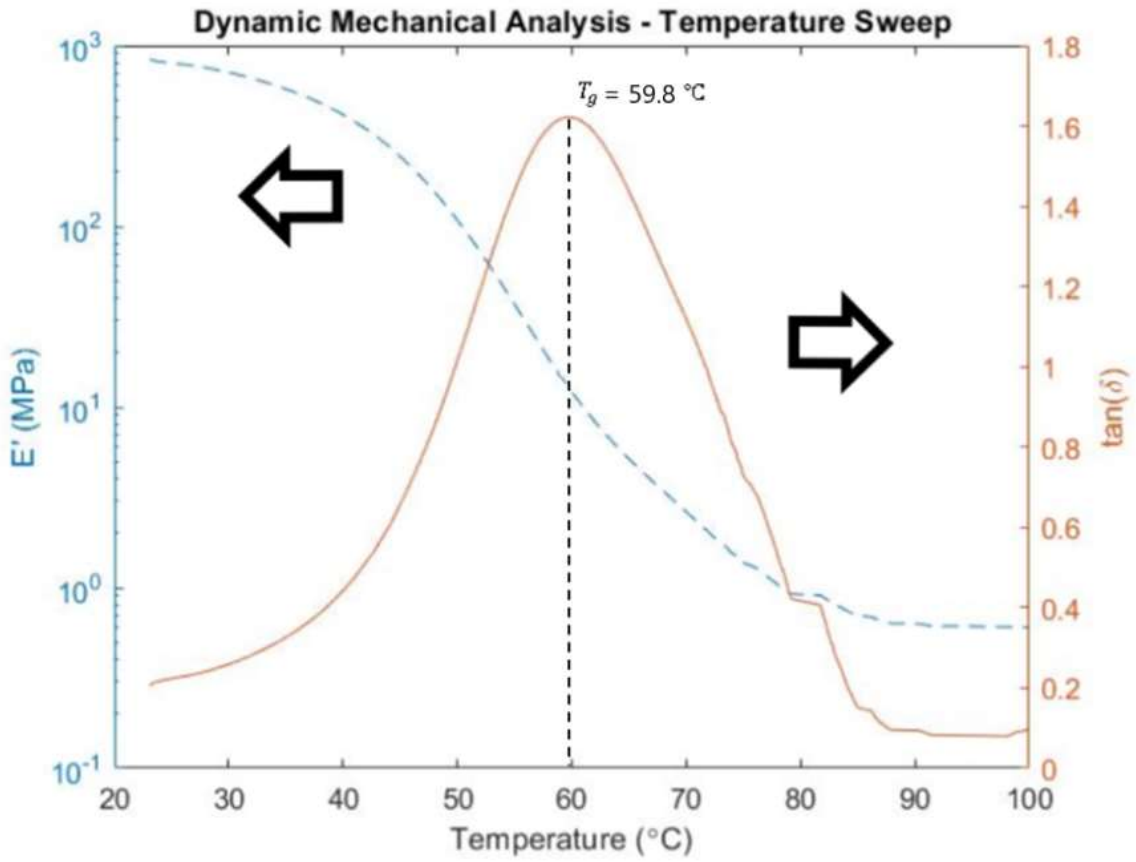

Figure 9: Storage Modulus behavior and tan(δ) across temperature

From the test, thermomechanical properties are investigated for the M-SMP samples, and T_g is measured to be 59.8 ℃ at the peak of the tan δ curve. As the temperature increases across the spectrum, the M-SMP decreases from 0.8 GPa to 0.6 MPa.

Chapter 4: Developing Functional Components

With a developed formulation capable of passing certain benchmark tests, it is imperative to be able to make the M-SMP precursor compatible with the custom DLP setup. What dictates the ability for the DLP printer to fabricate quality components with the precursor is through further optimization of parameters. Rather than formulation parameters as discussed in the previous chapter, it is through print process parameters that a functional product will be developed. As discussed in earlier sections, there exist many print process parameters which can be tuned to optimize the outcome of the print, but to maintain within scope and timeline of the project, only select parameters are tuned. Variable parameters include the exposure time of each layer to the light source. The base layer, layer that attached to the substrate on first iteration of printing, exposure time is also variable as it behaves separately from the "Nth" layer as well as dictates the ability to adhere to the substrate. The coordinate system orientation which a part is cured on also plays an important role in driving the quality and possibility of fabrication. For instance, a long rod in which the axis of the rod is printed in the z-direction (upwards), the results are much less favorable when compared to the same geometry printed on a rotated coordinate system.

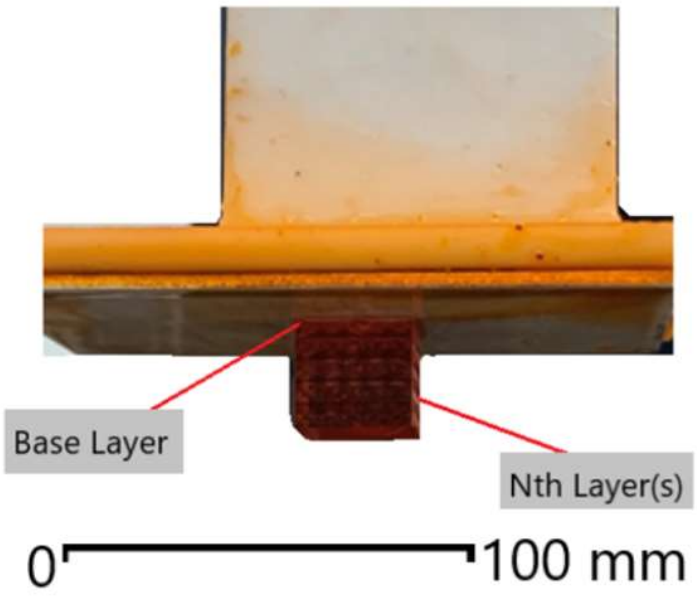

Figure 10: Diagram of relation of base layer to Nth layer

Like the process of the precursor formulation, a method of measuring success is needed in determining the success and quality of the fabricated components. One method of determining the success of DLP in printing the developed M-SMP precursor is in defining the target number of layers desired to print. The ability to print to a specified number of layers is a measure of success in terms of being able to extrude in the DLP's direction of translation. In terms of the quality of the printed structure of the XY-plane, quantitative measurements are taken and compared to model dimensions. Qualitatively, the printed parts are observed to note any defects or abnormalities not easily measured by measurement and testing devices.

Models developed are done so by targeting geometric design to emphasize features and limitations in varying complexities. The first geometry is a component where the actuation is limited to a single dimension. The beam structure is simple in its geometrical shape but is used to characterize the ability of magnetic actuation as well as shape locking. After testing a

cantilevered beam to observe behavior in a single dimension, a more complex shape is tested. The next geometry is used to demonstrate the actuation ability in the XY dimension. Also, the notched design and thin walls as well as height are designed to characterize a fuller extent of the DLP printing of the M-SMP resin.

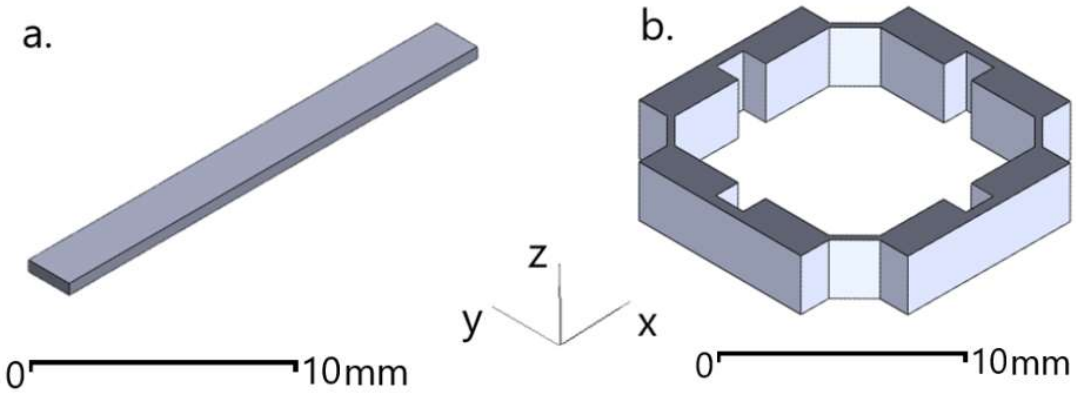

Figure 11: CAD render of DLP printed structures for a.) 1D actuation and b.) 2D actuation

By measuring the various dimensional values and comparing the results to the desired CAD model, the apparent quality of the printed part can be analyzed. To measure the dimensions in each axis, defining dimensions a caliper is used. However, the goal of the research is to be able to develop functional parts and establish a process where DLP can allow for small, functional parts made from the M-SMP. As such, the ability for the fabricated component to be actuated and respond to the external stimuli such as an applied magnetic field as well as temperature is important to determining the success and measurable ability of the material. Each feature of the printed structure's functionality is measured by demonstrating actuation in varying complexities of geometries.

Table 4: Results of critical print process parameters

Print Process Parameter	Value	Units
First Layer Exposure Time	20	[s]
Nth Layer Exposure Time	3	[s]
Motorized Stage Max Velocity	2	[mm/s]
Motorized Stage Acceleration	1	[mm/s^2]

Iterative testing was done to determine an appropriate set of print process parameters to produce functional and quality parts. The first layer is >6x longer than the Nth layer in terms of exposure time to develop a stable and strong bond with the first layers of the structure as well as the glass substrate. Below optimal timing produced prints with low bond fidelity.

For determining the Nth layer exposure time, the cure depth results were used to guide the parameter's value. As mentioned, since the layer thickness is constant at 0.05 mm, the critical cure depth needed to exceed double that (0.1 mm). A drawback of using too high of an exposure time is overcuring in the printed part resulting in poor quality or print lead times that are extremely high. At t = 3 s, a balance between these tradeoffs is made to not compromise the print quality.

The velocity and acceleration of the moving stage – consequently the substrate – is of high importance to the quality of the printed structure. While multifactorial, a high velocity of translation places the cured structure at risk of tearing interlayer bonds if not highly cured. Because there is some bonding force interaction from the PDMS tank as well as the cured resin, a high velocity has shown to destroy components during the printing process. As such, lower

velocities are used to print with higher confidence of success. The maximum velocity of the stage is 2 mm/s while the acceleration is only 1 millimeter per second per second.

Table 5: Comparison of CAD model and measured print dimensions

Model Type	CAD Dimensions (mm)			Measured Dimensions (mm)			(%) Deviation		
	x	y	z	x	y	z	x	y	z
1D	20.00	2.00	0.50	21.52	2.60	0.69	7.06	23.08	27.54
2D	18.60	18.60	1.50	20.42	20.65	1.48	8.91	9.93	1.35

In the images above, the thin beam (1D) is modeled with dimensions as noted in Table 5. After printing and subjecting the part to post-processing, the dimensions in each axis were measured. In the x-axis of the component (length), a percent deviation of length is found to be 7.06%. In both the height and width of the component, however, the true dimensions are significantly bigger in the range of approximately ~25% between the two. It can also be noted that the dimensions are extremely small on the order of less than 1 mm to 2 mm. This range and smaller produced the high deviations while the length dimension was found to be within some range of acceptability. This model when printed was split into 10 layers at 0.05 mm each layer.

Observing the 2D specimen, which has noticeably larger dimensions, the dimensions are seen to be overall closer to the desired value. Like the thin beam for the 1D specimen, the length and width (X and Y) are comparable in terms of deviation from desired CAD value at 8.91% and 9.93% deviation respectively for the 2D structure. Alternatively, the height of the 2D specimen from the CAD model is much nearer to the true value at 1.35%. The height being printed is also three times larger than the 1D model. In the 2D model, the thin-walls from the corner joints are also stable and near the model value. The structure is sliced into 30 individual layers and printed

at the specified 0.05 mm layer thickness. In both, no significant deformities or structural defects were present which allows the two parts to be tested in the actuation phase of validation testing.

While the dimensions of the part are relatively straightforward by measurement of calipers, the setup and testing of the actuation profile is slightly more complex. To set up the testing for actuation, a Helmholtz coil is used. To mimic the external magnetic field in a potential application for the M-SMP component, the test specimens are placed between two copper coils, and a current profile driving the magnetic field profile is also applied to the coils to generate a uniform magnetic field to actuate the magnetized part. The printed parts are not magnetic directly after printing. After each print, post-processing occurs by curing the structures at 80 degrees Celsius and in a UV chamber to ensure complete curing of any M-SMP resin material. After, the magnetization profile is determined which dictates the polarization. A large impulse generated by stored energy in capacitors then magnetizes the hard-magnetic NdFeB which permanently magnetizes them. This impulse magnetization produces the magnetic actuation ability based on orientation of the field and applied impulse 1.5 T magnetic field.

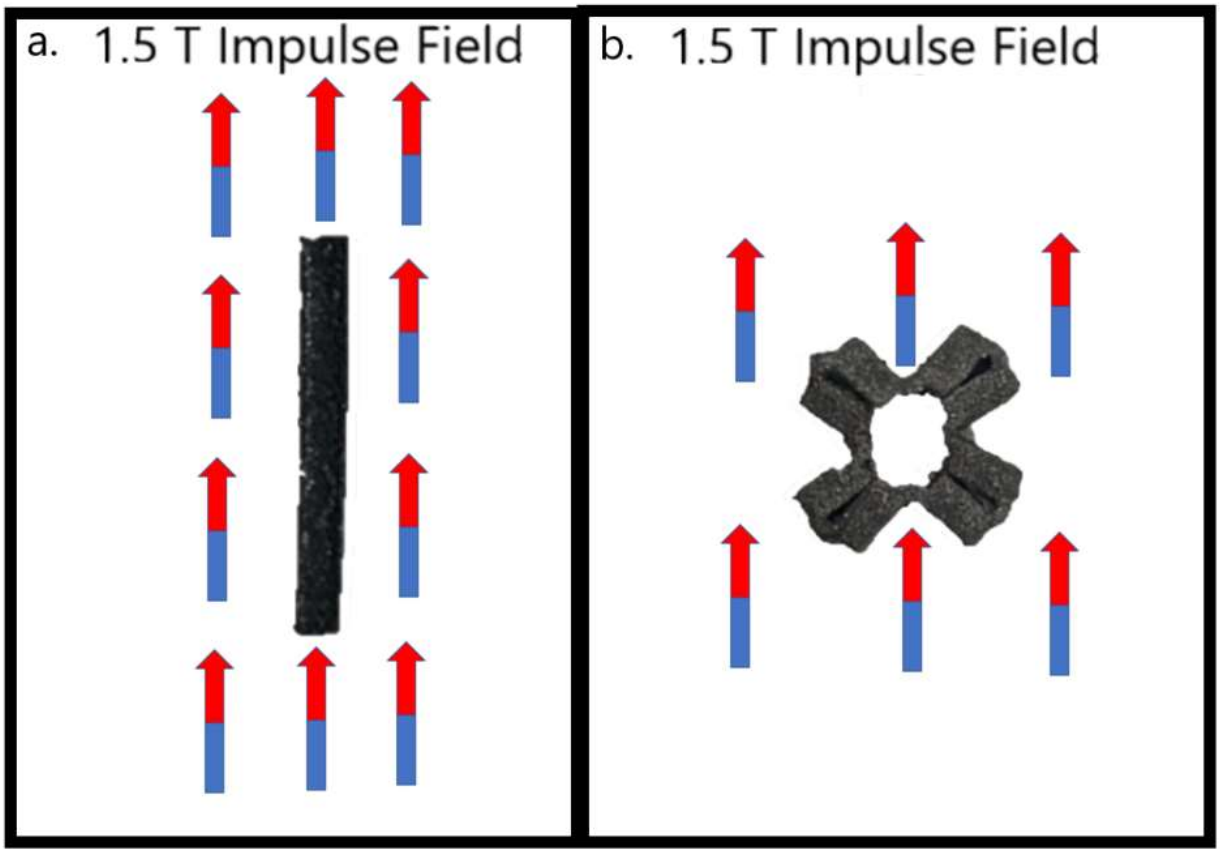

Figure 12: Magnetic Field orientation and structure configuration for a.) 1D actuation test piece and b.) 2D actuation test piece

With the magnetized specimens, the proper Helmholtz setup is needed to execute the actuation testing scheme for the one-dimensional actuation test. The specimen is kept at room temperature before the testing which is well below the glass transition temperature (T_g) at upwards of 60 degrees Celsius. Because of this, the structure is very stiff and will not bend prior to testing as seen in the image below. Also, due to the small mass, the bending due to gravity is minimized. The specimen is kept in this orientation as the magnetic field applied by the Helmholtz coils are directed in the upwards and downwards direction (along cylindrical cutout centerline). The specimen is also fixed to a test rig to prevent tipping from its own momentum during actuation creating a cantilevered beam with the y-dimension on the face of the rig.

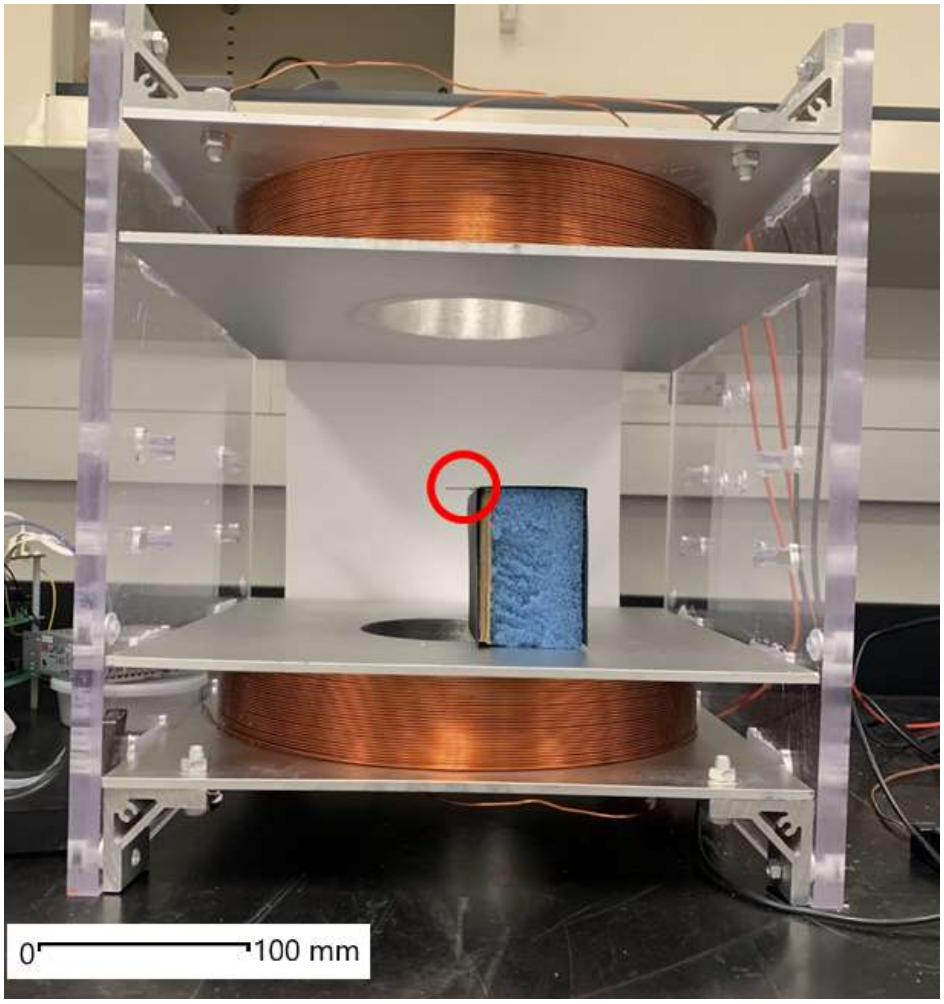

Figure 13: Setup of Helmholtz Coil and 1D test piece

The magnetic profile is also developed through the in-house software which controls the intensity and profile of the produced magnetic field through the current applied. The current applied is approximately 2.5 mT/A due to the distance between the coils.

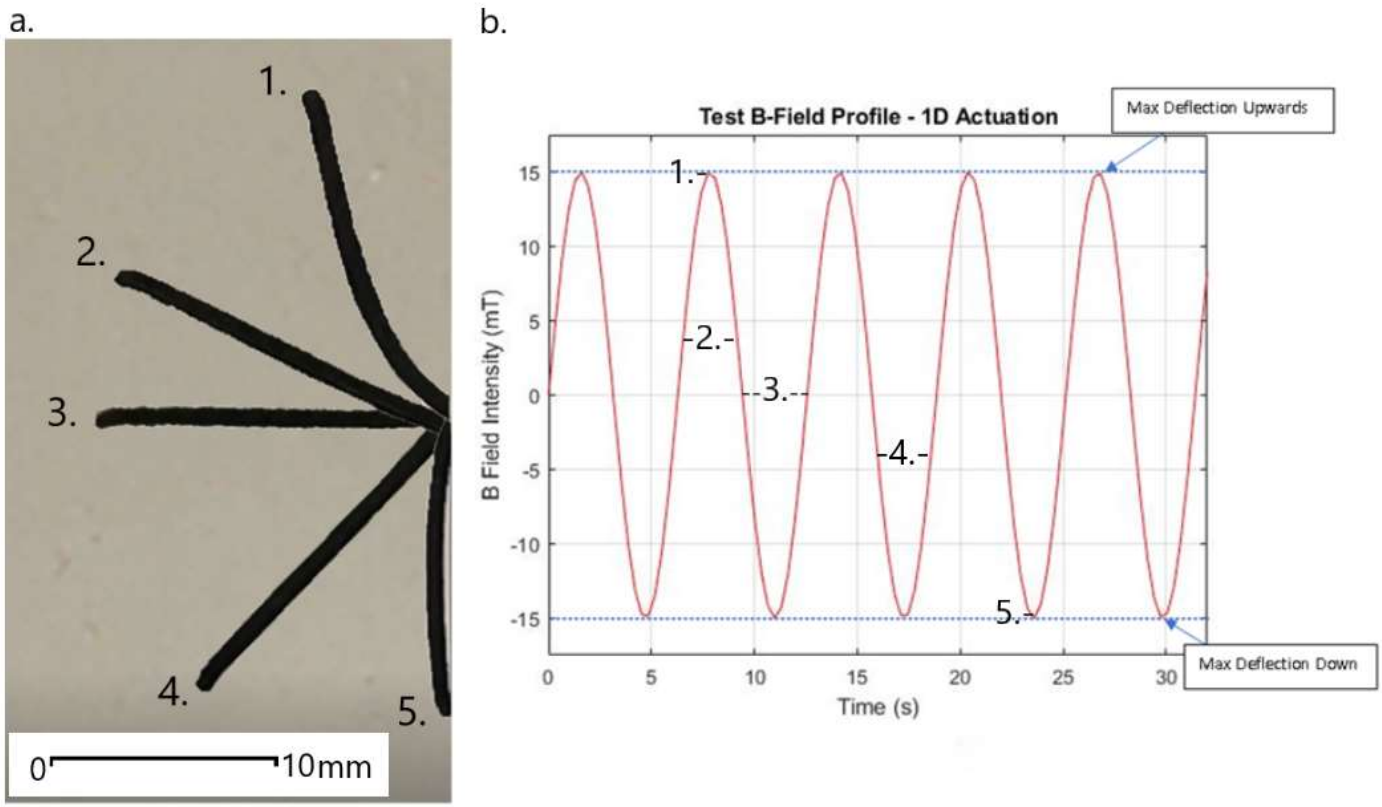

Figure 14: a.) Resulting intermediate positions of test piece with b.) associated magnetic profile for 1D actuation test

A sinusoidal profile is used for the one-dimensional test to show actuation and alignment of the magnetic fields in both directions as well as to demonstrate the ability for the printed part to exhibit shape-locking over time as it cools to below the glass transition temperature after being heated to well above it. Prior to executing the profile, a heat gun is used to heat the specimen to ~90 degrees Celsius to allow actuation and low stiffness in its rubbery state. During the test, a fan is used to blow ambient air at the specimen without disrupting the actuation to cool it down.

In Figure 14, the maximum deflection is observed in the positive (+ and -) maximum amplitude of the sine wave current profile as being upwards, and the opposite direction amplitude produces reversed aligning to the applied magnetic field. Since the beam is

cantilevered, only rotation is possible for motion. This is observed throughout the test as the beam orients in the upward and downwards direction. Each of the various positions caused from the applied magnetic field are shown (1. – 5.) in Fig. 14a and Fig. 14b as it completes a revolution. In the upward direction, slight gravitational effects do not allow the beam to flex as fully as in the downward position, but the trajectory of the beam shows movement freely above the initial position's axis.

Over the course of the test, the same profile is applied to the beam in a sinusoidal wave, but as it reaches nearer the glass transition temperature during cooling, the beam becomes stiffer.

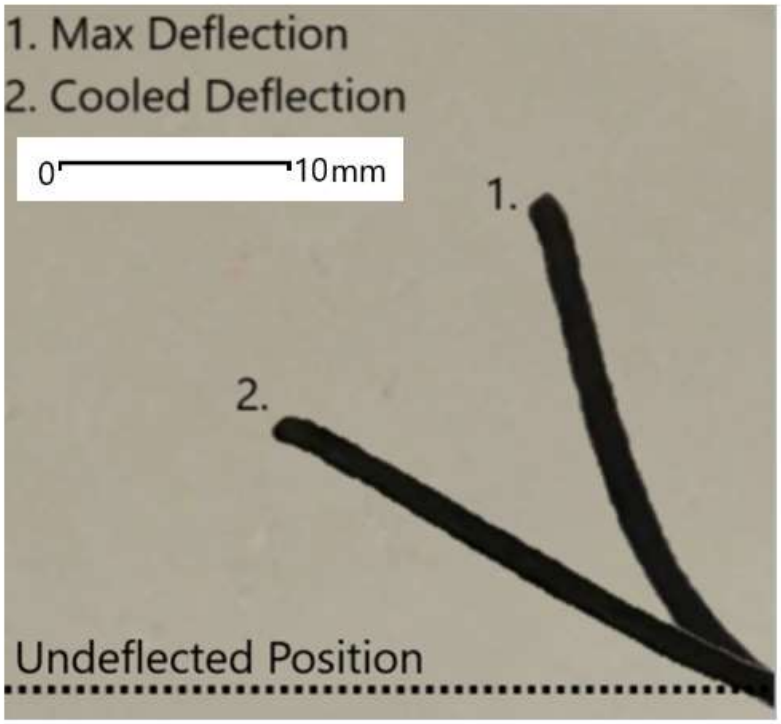

Position	Temperature (℃)	Storage Modulus (Mpa)	B Intensity (mT)
1.	~80	0.9	15
2.	~65	4.6	

Figure 15: Comparison of max deflection at various temperatures

Illustrated above is a depiction of the maximum deflections produced by the positive maximum amplitude. Initially, the angle of deflection is near 90 degrees relative to the starting orientation. Over time, as the forced convective cooling produced by the applied fans and removal from heat, the beam becomes stiffer resulting in resistance to deflection. The magnetic force from the maximum amplitude results in even less deflection (much less than 90 degrees). When comparing the storage moduli at each temperature, the cooler temperature results in a

much stiffer behavior (0.9 MPa) than the relatively more flexible state at above the glass transition (4.6 MPa).

In the following testing, the two-dimensional actuation is performed via the second model. The same Helmholtz coil is used in this test, but the rig is rotated 90 degrees to allow the specimen to rest its length and width onto a flat surface. This is done to align the magnetization of the specimen with the flat surface to allow minimum interference from gravity. This is caused due to the actuation in multiple dimensions, so the printed structure cannot be fixed in any way to the surface so that we can observe the behavior under magnetic and thermal stimulation. Below illustrates the changes made to the configuration of the test from the one-dimensional testing to the two-dimensional testing. Also, the printed structure is shown to highlight the changes in the placement of the surface and structure relative to where the magnetic field is applied.

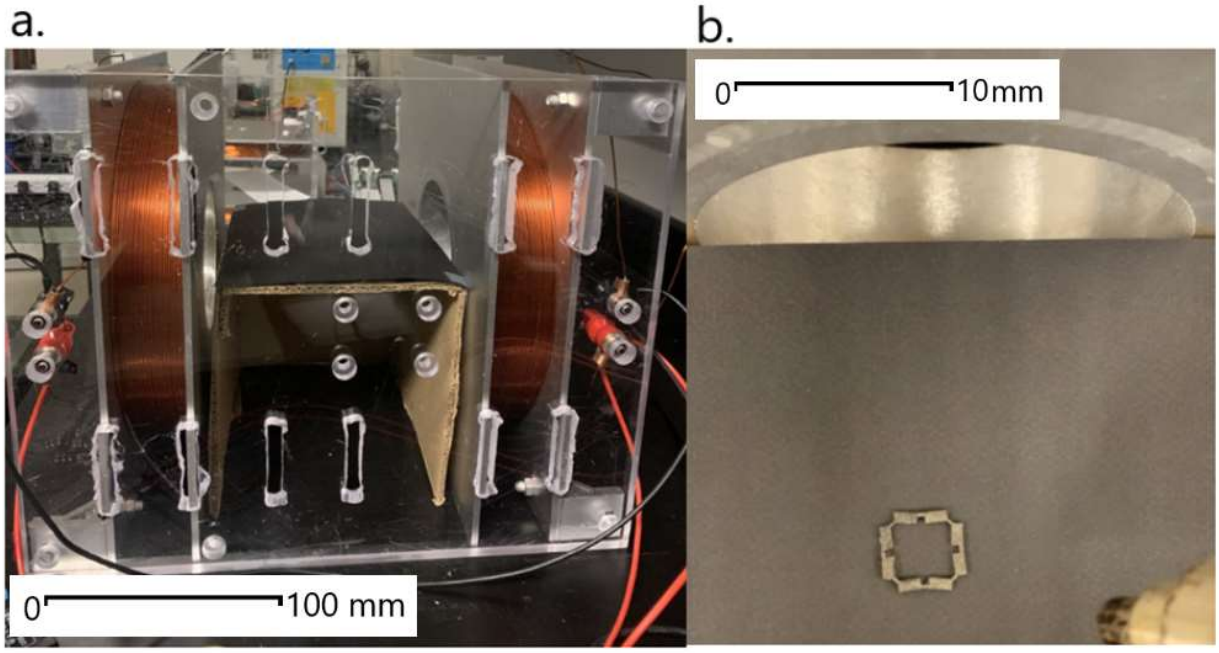

Figure 16: a.) Side profile of test setup of Helmholtz coil and b) top view of test piece for 2D actuation

For this test, the profile used is a ramp up to the maximum intensity (60 mT) where it is held at constant for 6 seconds before completing the test. Unlike the previous test, the profile does not produce opposing direction magnetic fields, and this was done so because the objective of this test was to observe the movement in the X and Y axes possible by the printed geometry.

A higher intensity than the previous test is also used to observe the maximum amount of deflection while in its rubbery state the geometry could withstand as a test of the actuation effectiveness and the geometric quality to allow the deflection. A heat gun is used in this test as well to heat the specimen to above its glass transition temperature and even during a short portion of the test because of the reduced effect of gravity on the actuation.

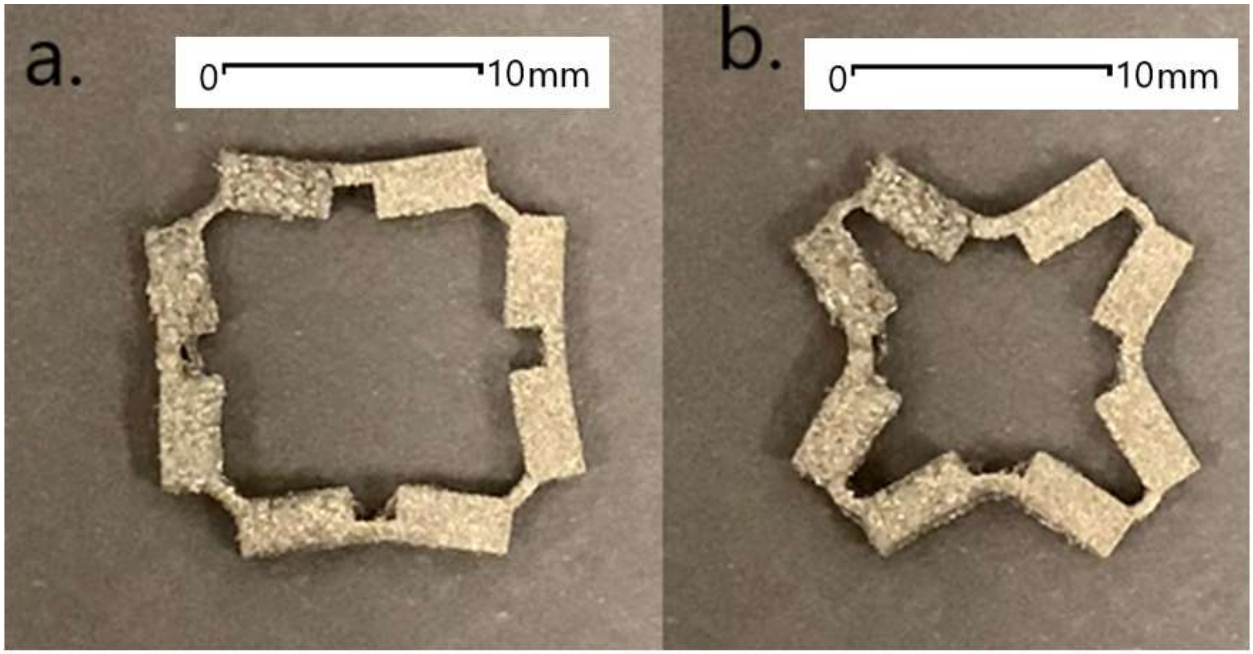

Figure 17: Comparison of a.) zero-deflection and b.) max deflection at above glass transition temperature

In the two-dimensional actuation tests, the magnetic field is ramped up to the maximum value to actuate the printed structure. Due to the nature of actuation while untethered, the printed part requires symmetrical interaction to not slip on itself. In this geometry, the desired actuation is to fold itself about each of its corner joints. The ideal shape is to configure itself in the same position as when impulse magnetized (45-degree angles on joints). The structure was able to successfully actuate uniformly in the planar directions, and the final configuration of the part is approximately the shape of the impulse magnetized shape.

Conclusion

The research project's intent was to enhance the capability of M-SMP by developing a method of manufacturing and corresponding print process parameters combined with compatible resin formulation. This is done do achieve capability of rapidly fabricating components on a millimeter-scale with higher complexity geometry than previously capable.

Contributions

Digital Light Processing as a unique method of fabricating M-SMP is transformative in that components can be fabricated at fractional times that that of some types of current fabrication methods. Additionally, the range of complexity allowable in a DLP-developed part is high as 3D geometries are simply projected onto the resin tank and cured.

Contributions to the field of smart materials are present in this project as high functionality materials are now combined simply and rapidly with complex geometries which allow the developed parts to exert unique control and actuation not previously capable as easily or readily.

Additional Applications

The outcomes of the research project include a vast array of applications. Because smart materials are an area of research gaining in attention, the ability to manufacture materials is something which has limited their functionality in the field. As a result, enabling DLP printing to manufacture components rapidly and conveniently with good resolution and speed enables those working with M-SMP to increase the degree of functionality. Area in which complex structures combined with smart materials can provide a great benefit is within the field of soft robotics.

Replacing rigid end effectors with dynamically configurable components from smart materials increases functional use of certain robotics applications.

The field of medicine also has various need for the application for alternatives to current materials and designs for eliminating invasive procedures. Drug delivery is an area of demonstrated promise, and the added complexity enabled by DLP produced M-SMP components only further adds to the possible treatments without the need for invasive surgeries.

Challenges

A variety of challenges arose during the project in areas such as setting up and calibration of the DLP system, formulation of the printable resin, and even in printing of the structures themselves.

Modifying the program to interact with the custom-built hardware required precise control and knowledge between the moving parts of the assembly such as the substrate and the translating stage. The MATLAB code also needed to reflect these interactions resulting in velocity and position studies to identify ways of developing a functioning printer design.

When formulating the printable resin, the sheer number of parameters influencing the quality of the resin required a focus and scoping of optimizable parameters for the sake of the timeline of the project.

During the print process itself, challenges arose in the material interactions from the resin, substrate, and even the resin tank. The commercial material, PDMS, proved to be problematic in its sustainability over the course of multiple prints as is degraded with just a few print cycles. This caused some investigation into mitigating this, and ultimately a solution was found to produce successful results.

Future Work

With the conclusion of this work, there are many avenues in which this work may progress. Having expanded capability to develop small, millimeter-scale, and complex parts, developing tools in areas of medicine and soft robotics can be researched and advanced further. Specifically, with M-SMP and DLP printing, further work can be done to fabricate components sustainably and more effectively with high levels of detail and taking advantage of the magnetic actuation with functional design of components. Improvements with respect to the custom nature of the DLP setup can be made to increase this capability. This involves further research into the substrate of the DLP system to better adhere and detach to the cured resin. Also, the resin tank can be made more effective through increased research into the detachment methods of the DLP system and to increase life cycle of the tank material.

With the application of this manufacturing method and through existing metamaterial research, tunable materials can be achieved [10]. The possibilities of application through developmental work in a rapid method of fabricating M-SMP also allows promising advancements in fields of soft robotics [11, 12, 23], biomedical applications [13], and more using programmable and configurable materials [14] like these.

Summary of Work

The research project took on a phased approach to developing what ultimately is a highly effective method of fabricating M-SMP. The approaches consisted of developing the custom hardware setup combined with the appropriate software to control the system to behave as a bottom-up DLP system. This included the print process parameters which were optimized to print specifically for M-SMP.

Once satisfied, the M-SMP needed to be developed into a compatible precursor with photosensitive capabilities. Through a series of experimental tests and material characterization, a photocurable resin that exhibits good cure depth, high precision dimensional accuracy was developed. From there, tunable print settings were optimized for the hardware through associated software application to demonstrate good printing capability. Structures in both the 1D and 2D were developed to characterize the quality and effectiveness of the prints and demonstrate the ability of combined material functionality with magnetic actuation as well as increasingly complex components.

Appendix

MATLAB Program for DLP Printer:

```
clear; close all; clc;

%%%%%%%%%%%%%%%%
%%%% INPUTS %%%%
%%%%%%%%%%%%%%%%

% Image file extension
fileType = '.png';

% Images folder location (note the slash at the end)
fileLocation = 'C:\Users\cruzb\OneDrive\Desktop\OSU 20-21\Research\Work\low_res.slice\';

% Image file prefix (do not include the numbers at the end)
fileName = 'low_res';

% Dark slice Images folder location (note the slash at the end)
fileLocation2 = 'C:\Users\cruzb\OneDrive\Desktop\OSU 20-21\Research\Work\Controlling&printing
Matlab\';

% Dark slice Image file prefix (do not include the numbers at the end)
fileName2 = 'dark slice';


% First Layer curing time
firstLayerTime = 30;%60; % seconds

% Nth Layer curing time
cureTime = 5;%23;%26; % seconds

% Total distance traveled for offset downward
offset = 2; % mm

% Print Layer thickness
layerThick = 0.05;%0.075; % mm

% Number of layers or the number of images in your image folder
numberOfLayers = 261;


%%%%%%%%%%%%%%%%%%
%%%% END INPUTS %%%%
%%%%%%%%%%%%%%%%%%

global h; % make h a global variable so it can be used outside the main
% function. Useful when you do event handling and sequential           move
```

Create Matlab Figure Container

```
fpos    = get(0,'DefaultFigurePosition'); % figure default position
fpos(3) = 650; % figure window size;Width
fpos(4) = 450; % eight

f = figure('Position', fpos,...
    'Menu','None',...
    'Name','APT GUI');
```

Create ActiveX Controller

```
h = actxcontrol('MGMOTOR.MGMotorCtrl.1',[20 20 600 400 ], f)
```

Initialize

Start Control

```
h.StartCtrl;

% Set the Serial Number
SN = 45995880; % put in the serial number of the hardware
set(h,'HWSerialNum', SN);

% Indentify the device
h.Identify;

pause(5); % waiting for the GUI to load up;
```

Event Handling

```
h.registerevent({'MoveComplete' 'MoveCompleteHandler'});
```

Loop

```
pause(1);

countLayers = numberOfLayers-1;

fprintf('Printing Started...\n');

filename2 = strcat(fileLocation2, 'dark slice',fileType);
image2 = imread(filename2);
fullscreen(image2, 1);

pause(10);

startTime=tic;
```

```
startPos = h.GetPositionEx_UncalibPosition(0);

for i=0:countLayers

    if i < 10
        prefix = strcat(fileName,'000');
    elseif i < 100
        prefix = strcat(fileName,'00');
    elseif i < 1000
        prefix = strcat(fileName,'0');
    end
    iString = int2str(i);

    layerString = strcat('Layer ',iString, '\n');
    fprintf(layerString);

    filename = strcat(fileLocation, prefix, iString, fileType);
    image = imread(filename);
    fullscreen(image, 1);
    fprintf('image on \n')

    if i == 0
        pause(firstLayerTime);

    else
    pause(cureTime);
    end


    filename2 = strcat(fileLocation2, 'dark slice',fileType);
    image2 = imread(filename2);
    fullscreen(image2, 1);
    fprintf('image off \n')

    % Offset Drop Down %
    h.MoveAbsoluteEx(0,startPos-(i)*layerThick-offset,0,1);
    %pause(2);
    h.MoveAbsoluteEx(0,startPos-(i)*layerThick,0,1);
    pause(2);
end


fprintf('Print Complete... Moving to Home \n');
%h.MoveHome(1,true)
h.StopCtrl;
%closescreen();
```

Bibliography

1. Xie, Tao. “Tunable Polymer Multi-Shape Memory Effect.” *Nature*, vol. 464, no. 7286, Mar. 2010, pp. 267–70, doi:10.1038/nature08863.
2. Shuai Wu *et al* 2020 *Multifunct. Mater.* **3** 042003
3. Ze, Qiji, et al. “Magnetic Shape Memory Polymers with Integrated Multifunctional Shape Manipulation.” *Advanced Materials*, vol. 32, no. 4, John Wiley & Sons, Ltd, Jan. 2020, p. 1906657, doi:10.1002/adma.201906657.
4. Ma, Chunping, et al. “Magnetic Multimaterial Printing for Multimodal Shape Transformation with Tunable Properties and Shiftable Mechanical Behaviors.” *ACS Applied Materials & Interfaces*, vol. 13, Sept. 2020, doi:10.1021/acsami.0c13863.
5. Wallin, T. J., et al. “3D Printing of Soft Robotic Systems.” *Nature Reviews Materials*, vol. 3, no. 6, June 2018, pp. 84–100, doi:10.1038/s41578-018-0002-2.
6. Truby, Ryan L., and Jennifer A. Lewis. “Printing Soft Matter in Three Dimensions.” *Nature*, vol. 540, no. 7633, Dec. 2016, pp. 371–78, doi:10.1038/nature21003.
7. Mantada, Phaneendra, et al. “Parameters Influencing the Precision of Various 3D Printing Technologies.” *MM Science Journal*, vol. 2017, Dec. 2017, pp. 2004–12, doi:10.17973/MMSJ.2017_12_201776.
8. Wintech Digital Systems Technology Corporation. (2015). *DLP PRO4500 User’s Guide.* Retrieved from http://www.windlp.com/upload/file/201703/20170302113948_49951.pdf
9. Shen, Beijun, et al. “Programming the Time into 3D Printing: Current Advances and Future Directions in 4D Printing.” *Multifunctional Materials*, vol. 3, Nov. 2019, doi:10.1088/2399-7532/ab54ea.
10. Montgomery, S. M., Wu, S., Kuang, X., Armstrong, C. D., Zemelka, C., Ze, Q., Zhang, R., Zhao, R., Qi, H. J., Magneto-Mechanical Metamaterials with Widely Tunable Mechanical Properties

and Acoustic Bandgaps. *Adv. Funct. Mater.* 2021, 31, 2005319. https://doi.org/10.1002/adfm.202005319

11. Zhang, Hang, et al. "Soft Mechanical Metamaterials with Unusual Swelling Behavior and Tunable Stress-Strain Curves." *Science Advances*, vol. 4, no. 6, June 2018, p. eaar8535, doi:10.1126/sciadv.aar8535.
12. Liu, Ying, et al. "Sequential Self-Folding of Polymer Sheets." *Science Advances*, vol. 3, no. 3, Mar. 2017, p. e1602417, doi:10.1126/sciadv.1602417.
13. Kim, Yoonho, et al. "Ferromagnetic Soft Continuum Robots." *Science Robotics*, vol. 4, no. 33, Aug. 2019, p. eaax7329, doi:10.1126/scirobotics.aax7329.
14. Lum, Guo Zhan, et al. "Shape-Programmable Magnetic Soft Matter." *Proceedings of the National Academy of Sciences*, vol. 113, no. 41, Oct. 2016, p. E6007, doi:10.1073/pnas.1608193113.
15. Liao, G. J., et al. "Development of a Real-Time Tunable Stiffness and Damping Vibration Isolator Based on Magnetorheological Elastomer." *Journal of Intelligent Material Systems and Structures*, vol. 23, no. 1, SAGE Publications Ltd STM, Dec. 2011, pp. 25–33, doi:10.1177/1045389X11429853.
16. Kokkinis, Dimitri, et al. "Multimaterial Magnetically Assisted 3D Printing of Composite Materials." *Nature Communications*, vol. 6, no. 1, Oct. 2015, p. 8643, doi:10.1038/ncomms9643.
17. Chen, Kaijuan, et al. "Dynamic Photomask-Assisted Direct Ink Writing Multimaterial for Multilevel Triboelectric Nanogenerator." *Advanced Functional Materials*, vol. 29, no. 33, John Wiley & Sons, Ltd, Aug. 2019, p. 1903568, doi:10.1002/adfm.201903568.
18. Matsuzaki, Ryosuke, et al. "Multi-Material Additive Manufacturing of Polymers and Metals Using Fused Filament Fabrication and Electroforming." *Additive Manufacturing*, vol. 29, Oct. 2019, p. 100812, doi:10.1016/j.addma.2019.100812.

19. Mansouri, M. R., et al. “3D-Printed Multimaterial Composites Tailored for Compliancy and Strain Recovery.” *Composite Structures*, vol. 184, Jan. 2018, pp. 11–17, doi:10.1016/j.compstruct.2017.09.049.

20. Loke, Gabriel, et al. “Structured Multimaterial Filaments for 3D Printing of Optoelectronics.” *Nature Communications*, vol. 10, no. 1, Sept. 2019, p. 4010, doi:10.1038/s41467-019-11986-0.

21. Roach, Devin J., et al. “The M4 3D Printer: A Multi-Material Multi-Method Additive Manufacturing Platform for Future 3D Printed Structures.” *Additive Manufacturing*, vol. 29, Oct. 2019, p. 100819, doi:10.1016/j.addma.2019.100819.

22. Sungwoong Jeon, Ali Kafash Hoshiar, Kangho Kim, Seungmin Lee, Eunhee Kim, Sunkey Lee, Jin-young Kim, Bradley J. Nelson, Hyo-Jeong Cha, Byung-Ju Yi, and Hongsoo Choi. *Soft Robotics*.Feb 2019.54-68.http://doi.org/10.1089/soro.2018.0019

23. Ge, Qi, et al. “Multimaterial 4D Printing with Tailorable Shape Memory Polymers.” *Scientific Reports*, vol. 6, no. 1, Aug. 2016, p. 31110, doi:10.1038/srep31110.

24. Miri, Amir K., et al. “Microfluidics-Enabled Multimaterial Maskless Stereolithographic Bioprinting.” *Advanced Materials*, vol. 30, no. 27, John Wiley & Sons, Ltd, July 2018, p. 1800242, doi:10.1002/adma.201800242.

25. Han, Daehoon, et al. “Rapid Multi-Material 3D Printing with Projection Micro-Stereolithography Using Dynamic Fluidic Control.” *Additive Manufacturing*, vol. 27, May 2019, pp. 606–15, doi:10.1016/j.addma.2019.03.031.

26. Meng, Harper, and Guoqiang Li. “A Review of Stimuli-Responsive Shape Memory Polymer Composites.” *Polymer*, vol. 54, no. 9, Apr. 2013, pp. 2199–221, doi:10.1016/j.polymer.2013.02.023.

27. Patel, Dinesh K., et al. “Highly Stretchable and UV Curable Elastomers for Digital Light Processing Based 3D Printing.” *Advanced Materials*, vol. 29, no. 15, John Wiley & Sons, Ltd, Apr. 2017, p. 1606000, doi:10.1002/adma.201606000.

28. Novelino, Larissa S., et al. “Untethered Control of Functional Origami Microrobots with Distributed Actuation.” *Proceedings of the National Academy of Sciences*, vol. 117, no. 39, Sept. 2020, p. 24096, doi:10.1073/pnas.2013292117.